GREEN'S FUNCTION APPROACH TO THE RAPID PREDICTION OF THERMOACOUSTIC INSTABILITIES IN COMBUSTORS

Alessandra Bigongiari

Faculty of Natural Sciences, Keele University, Keele, ST55BG Staffordshire, UK
Dipartimento di Fisica, Università di Pisa, Largo Bruno Pontecorvo 3,56127, Pisa, Italy
email: a.bigongiari@keele.ac.uk

Maria Heckl

Faculty of Natural Sciences, Keele University, Keele, ST55BG Staffordshire, UK

Dmytro Iurashev

Università degli Studi di Genova, DICCA, via Montallegro 1, 16145

The prediction of thermo-acoustic instabilities is fundamental for combustion systems such as industrial gas turbine engines. High-amplitude pressure oscillations, also known as humming, cause thermal and mechanical stress to the equipment leading to premature wear or even critical damage. In order to operate a combustion system safely, it is necessary to know its stability boundaries for the conditions under which it is expected to operate. Finding the operation boundaries based on trial and error is risky and expensive. 3D simulations can provide details on heat transfer and flow structures, but demand large computational efforts due to the multi-scale nature of combustion problems, and are not suited for parametric studies. In this article we use a 1D Green's function approach to map the stability of a BRS (Beschaufelter Ring-Spalt) burner as a function of different parameters and boundary conditions. The burner is modelled as a 1D system where the flame is described by a Flame Describing Function (FDF) and boundary conditions are described through reflection coefficients. The method is able to provide rapid predictions on the stability behaviour of the system while giving a fundamental insight into the physical mechanism which is driving the instability.

1. Introduction

In the past decade, increased environmental awareness has resulted in the demand for the development of combustion systems with reduced emission of pollutants, in particular CO_2 and NO_x. Modern combustion concepts satisfy the low-emission requirement by operating with premixed flames in the lean regime. However, this set-up brings a new problem: its implementation makes a combustion system more susceptible to thermoacoustic instabilities, and these can occur suddenly and spontaneously. These are generated by a feedback mechanism between a heat source characterized by a fluctuating heat release rate and the acoustic field in the burner.

There are several approaches to the prediction of combustion instabilities [1]. One approach consists on the use of low-order models, in which the combustor system is divided into series of simpler subsystems and mathematical transfer function matrices are used to connect lumped acoustic elements to each other. Another approach is to perform CFD simulations to model directly the interaction between combustion, acoustics and flow. The latter can be computationally expensive:

combustion modelling is a multiscale problem, with length scales ranging from less than 1 mm (flame front thickness) to more than 1 m (acoustic wavelength). In addition, the frequency to growth-rate ratio can be very large for an acoustic disturbance; this means that an unsteady CFD simulation of a slowly growing instability would necessitate the simulation of a large number of cycles, with high temporal accuracy. For parametric studies it is advantageous to have some analytical model, which describes the combustion system in terms of a few parameters and captures the key physical aspects. In this paper we present a stability analysis of the BRS (Beschaufelter Ring-Spalt) burner where we use a nonlinear analytical approach based on the Green's function. The modeled set-up corresponds to an atmospheric swirl-stabilised burner where methane is burnt in the lean combustion regime.

Instabilities in fluid dynamics are typically described by governing equations in the form of coupled differential equations. We side-step them by turning our governing equations into a delay *integral* equation by using an approach based on the tailored Green's function. We will then illustrate that this can be solved with simple techniques, giving stability predictions quickly and without much numerical effort.

2. The Green's function approach

The Green's function is the acoustic field generated in the tube at location x and time t by an impulsive point source located at x' and firing at t'. We denote it by $G(x, x', t, t)$ and describe it in terms of the velocity potential. Its governing equation is the non-homogeneous wave equation,

$$\frac{1}{c^2}\frac{\partial^2 G}{\partial t^2} - \frac{\partial^2 G}{\partial x^2} = \delta(x-x')\delta(t-t') \; , \tag{1}$$

together with boundary conditions described by reflection coefficients R_0 at the inlet and R_L at the outlet. The Green's function is a superposition of modes, with modal amplitudes g_n and modal frequencies ω_n,

$$G(x,x',t,t') = H(t-t')\Im\sum_{n=1}^{\infty} g_n(x,x')e^{-i\omega_n(t-t')} \; . \tag{2}$$

$H(t-t')$ denotes the Heaviside function. The quantities g_n and ω_n are calculated analytically for the specific set-up of the BRS burner.

2.1 The modelled configuration

The BRS set-up consists of a cylindrical burner tube (diameter 40 mm, length 16 cm), which is connected to a square combustion chamber (cross-section $90 \times 90 \; mm^2$, length 30 cm). A central rod (diameter 16 mm, length 16 cm), which spans the length of the burner tube, acts as a bluff body and makes the burner tube effectively annular. A swirler with 8 blades is mounted on the central rod. The BRS test rig was initially developed by [2] at the Technische Universität München, and has been studied by different authors both experimentally [2] and numerically [3].

In order to apply the Greens' function approach to the BRS burner, we consider the idealized set-up shown in Figure 1. The burner tube is described as tube of constant cross-section S_1, with constant temperature $\overline{T}_1$; the combustion chamber has a larger cross-section S_2, and a constant temperature $\overline{T}_2 > \overline{T}_1$. The swirler is ignored; this is justified by the 3-D numerical simulations in [4] which show that the swirler does not influence the acoustic field significantly. We assume that the flame is compact and located at position $x_{q,}$; this is downstream of the burner exit plane, which is located at x_j. In the burner tube, the speed of sound is c_1, and the mean density is $\bar{\rho}_1$. In the hotter combustion chamber, they are c_2 and $\bar{\rho}_2$. The choice of this temperature distribution was based on [5], where it is shown that modelling the temperature gradient of the compact flame does not produce significant changes in the results with respect with a temperature jump. The boundary conditions at the tube

ends are described by the reflection coefficients R_0 at the inlet and R_L at the outlet, which account for losses.
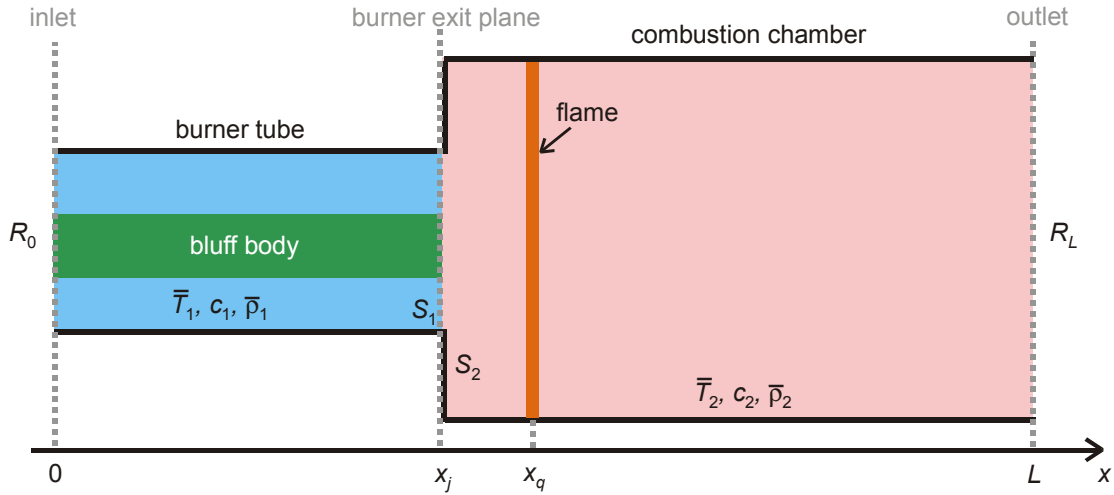
Figure 1: Schematic of the one-dimensional combustor under consideration.

2.2 Analytical form of the Green's function

The expression of the modal amplitudes g_n in the Green's function of Eq. (2) have been calculated for the configuration described in section 2.1 (see [5,13] for details on the derivation procedure); the results are

$$g_n(x,x') = i \frac{\hat{g}(x,x',\omega_n)}{2\omega_n F(\omega_n)} \Bigg|_{\substack{x=x_q \\ x'=x_q}} , \tag{3}$$

with

$$\hat{g}(x,x',\omega) = \begin{cases} D(x,\omega)C(x',\omega) & \text{for } x_j < x < x_q \\ C(x,\omega)D(x',\omega) & \text{for } x' < x < L \end{cases} \tag{4}$$

and

$$C(x,\omega) = e^{i\frac{\omega}{c_2}(x-L)} + R_L e^{-i\frac{\omega}{c_2}(x-L)}, \tag{5a}$$

$$D(x,\omega) = \frac{S_{ratio}}{2} \frac{c_2}{c_1} (R_0 e^{i\omega\frac{x_q}{c_1}} - e^{-i\omega\frac{x_j}{c_1}})(e^{i\frac{\omega}{c_2}(x-x_j)} - e^{-i\frac{\omega}{c_2}(x-x_j)})$$

$$+ \frac{1}{2} \frac{\bar{\rho}_1}{\bar{\rho}_2} (R_0 e^{i\omega\frac{x_q}{c_1}} + e^{-i\omega\frac{x_j}{c_1}})(e^{i\frac{\omega}{c_2}(x-x_j)} + e^{-i\frac{\omega}{c_2}(x-x_j)}). \tag{5b}$$

$$F(\omega) = \frac{S_{ratio}}{2} \frac{1}{c_1} [i(R_0 e^{i\omega\frac{x_j}{c_1}} - e^{-i\omega\frac{x_j}{c_1}})(e^{i\omega\frac{x_j-L}{c_2}} + R_L e^{-i\omega\frac{x_j-L}{c_2}})$$

$$- i\frac{c_1}{c_2} \frac{\bar{\rho}_1}{\bar{\rho}_2}(e^{i\omega\frac{x_j-L}{c_2}} - R_L e^{-i\omega\frac{x_j-L}{c_2}})(R_0 e^{i\omega\frac{x_j}{c_1}} + e^{-i\omega\frac{x_j}{c_1}})]. \tag{6}$$

$F(\omega)$ is the characteristic function, and the equation $F(\omega) = 0$ determines the modal frequencies ω_n in the Green's function. $S_{ratio} = S_1 / S_2$ is the ratio of cross-sectional areas.

2.3 The integral governing equation

The velocity potential $\phi(x,t)$ of a sound field generated by a heat source with heat release rate $q(x,t)$ (per unit mass), can be described by the acoustic analogy equation

$$\frac{1}{c^2}\frac{\partial^2 \phi}{\partial t^2} - \frac{\partial^2 \phi}{\partial x^2} = -\frac{\gamma-1}{c^2}q(x,t) \, , \tag{7}$$

together with the initial conditions

$$\phi(x,t)\big|_{t=0} = \varphi_0 \delta(x-x_q) \quad \text{and} \quad \frac{\partial \phi(x,t)}{\partial t}\bigg|_{t=0} = \varphi'_0 \delta(x-x_q) . \tag{8}$$

This set of equations can be converted into an integral equation for the acoustic velocity u with the use of the Green's function. For a compact source at $x = x_q$, described by

$$q(x,t) = q(t)\delta(x-x_q), \tag{9}$$

the integral equation is (see [13])

$$u_q(t) = \frac{\partial \phi}{\partial x}\bigg|_{x=x_q} = -\frac{\gamma-1}{c^2}\int_{t'=0}^{t}\frac{\partial G(x,x',t,t')}{\partial x}\bigg|_{\substack{x=x_q\\x'=x_q}}q(t')dt' - \frac{\varphi_0}{c^2}\frac{\partial G}{\partial x \partial t'}\bigg|_{\substack{x=x_q\\x'=x_q\\t'=0}} + \frac{\varphi'_0}{c^2}\frac{\partial G}{\partial x}\bigg|_{\substack{x=x_q\\x'=x_q\\t'=0}} . \tag{10}$$

It is worth noting that (10) is equivalent to the set of governing equations comprising (7), (8), and the boundary conditions described by R_0 and R_L. Equation (10) has a clear physical explanation: the heat release $q(t)$, which can be seen as a series of impulses covering the time interval $t' = 0,\ldots t$, generates an acoustic velocity, which is the sum of responses to the individual impulses. We also note that equation (10) is valid for both linear and nonlinear thermoacoustic systems.

3. Model for the heat release rate

In order to calculate the acoustic velocity from (10), we need an expression for the rate of heat release in terms of the acoustic field. Following Heckl [14], we use a generalized $n\tau$-law,

$$\frac{Q(t)}{\bar{Q}} = n_1 \frac{u_q(t-\tau)}{\bar{U}} - n_0 \frac{u_q(t)}{\bar{U}} , \tag{11}$$

where Q is the global heat release rate, $\bar{Q}$ is its mean value, and $\bar{U}$ is the mean flow velocity. τ is the time-lag that characterizes the response of the flame, and n_1, n_0 are coupling constants. The time-lagged term $u(t-\tau)$ describes the convective effects along the flame surface, and the direct-feedback term $u(t)$ describes heat losses at the flame base where convection plays no role [12].

In many practical premixed combustion systems individual particles travel slightly different distances and reach the flame front with slightly different delay times. This effect can be incorporated by introducing a time-lag distribution $D(\tau - \tau_c)$, centered on τ_c. Equation (11) then becomes

$$\frac{Q'(t)}{\bar{Q}} = n_1 \int_{\tau=0}^{\infty} \frac{u_q(t-\tau)}{\bar{u}} D(\tau - \tau_c)\, d\tau - n_0 \frac{u_q(t)}{\bar{u}} . \tag{12}$$

Time-lag distributions have been considered in several earlier flame models [6,7]. Unlike the discrete time-lag model (11), distributed time-lag models can explain the low-pass filter behaviour that is usually observed in measured flame transfer functions; moreover, a time-lag distribution can account for convective processes [7]. Here we use a Gaussian distribution with standard deviation σ,

$$D(\tau) = \frac{2}{\sigma\sqrt{2\pi}}e^{-\frac{\tau^2}{2\sigma^2}} . \tag{13}$$

We can write a *local* heat release law based on equation (12) as follows

$$q(t) = K \left[n_1 \int_{\tau=0}^{\infty} u_q(t-\tau)D(\tau-\tau_c)d\tau - n_0 u_q(t) \right], \tag{14}$$

where

$$K = \frac{\overline{Q}}{\overline{U}_2 S_2 \overline{\rho}_2} \tag{15}$$

is the heater power per mass flow, having units Wskg^{-1}.

3.1 Derivation of the heat release law through the Flame Describing Function (FDF)

The FDF is the response of the flame to a perturbation having a given frequency and amplitude; it relates the normalized fluctuations of the heat release to the normalized fluctuations of the acoustic velocity at a reference position upstream the flame:

$$\text{FDF}(A,\omega) = \frac{q(A,\omega)/\overline{Q}}{u'(A,\omega)/\overline{U}} . \tag{16}$$

The FDF can be obtained experimentally by applying a harmonic perturbation at the inlet (usually through a loudspeaker or a siren) and recording the time series of the acoustic velocity and heat release rate fluctuations. Spectral analysis then allows the derivation of the gain and phase of the flame response as a function of the perturbation amplitude and frequency (see [8]). This experimental procedure can be mimicked by full CFD simulation.

The inclusion of the amplitude-dependence is fundamental to the modelling of nonlinear effects, such as the formation of limit cycles. Our approach represents an advance compared with early nonlinear models, where an artificial saturation amplitude was imposed in order to "predict" limit cycles [10].

3.2 Modal analysis

The Green's function contains the information on the system parameters such as the tube geometry, temperature and end conditions, but it does not contain any information on the parameters that characterize the thermoacoustic feedback loop. The aim of this section is to determine the stability behaviour of individual acoustic modes in the *presence* of feedback. To this end, we express the acoustic velocity as a sum of modes with complex amplitudes u_m and complex frequencies Ω_m,

$$u_q(t) = \sum_{m=1}^{\infty} \left(u_m e^{-i\Omega_m t} + u_m^* e^{i\Omega_m^* t} \right) . \tag{17}$$

u_m and Ω_m are unknown at this stage; their complex conjugate is denoted by *. It is possible to determine them from a series of mathematical manipulations, based on the integral equation (10), the local heat release rate $q(t)$ in Eq. (14), and the modal expression for the Green's function in Eq. (2). We report here the equations for these two quantities that were obtained in [11] and extended to include the time-lag distribution. The equation for the frequencies Ω_m is

$$(n_1 \int_{\tau=0}^{\infty} e^{i\Omega_m \tau} D(\tau-\tau_c)d\tau - n_0) \sum_{n=1}^{\infty} \left[\frac{G_n}{i(\omega_n - \Omega_m)} - \frac{G_n^*}{i(\omega_n^* + \Omega_m)} \right] = -\frac{2c^2}{K(\gamma-1)}, \tag{18}$$

with G_n given by

$$G_n = \left. \frac{\partial g_n(x,x')}{\partial x} \right|_{\substack{x=x_q, \\ x'=x_q}} \tag{19}$$

and the equation for u_m is

$$\sum_{m=1}^{\infty}\left[u_m\frac{(-n_1\int_{\tau=0}^{\infty}e^{i\Omega_m\tau}D(\tau-\tau_c)d\tau+n_0)}{i(\omega_n-\Omega_m)}+u_m^*\frac{(-n_1\int_{\tau=0}^{\infty}e^{-i\Omega_m^*\tau}D(\tau-\tau_c)d\tau+n_0)}{i(\omega_n+\Omega_m^*)}\right]=\frac{i\omega_n\varphi_o+\varphi_0'}{K(\gamma-1)},\qquad(20)$$

as well as the complex conjugate of (20). Once (18) has been solved for Ω_m, the solution can be put into (20) to obtain the solution for the velocity amplitudes u_m.

Equations (18) and (20) show that the eigenmodes of the thermoacoustic system depend also on the parameters in the heat release model, in particular on the heater power K, the coupling constants n_0 and n_1, and implicitly through $D(\tau)$, on the parameters τ_c and σ in the time-lag distribution. We call these eigenmodes the *heat-driven modes* of the system and their frequencies the *heat-driven frequencies*. Unless the feedback is missing, Ω_m and ω_m differ both in real and imaginary part. The shift in real part is generally non-negligible (see [11]); this is a consequence of the thermoacoustic feedback. The imaginary part of Ω_m gives the stability behaviour of the heat-driven mode m.

4.   Stability maps

In this section we investigate the stability behaviour of the first heat-driven mode Ω_1. The configuration in section 2.1 is described analytically by the Green's function in section 2.2, and the flame is described by a heat release law of the form (14) with amplitude-dependent parameters:

$$n_0 = 0.408 - 0.186A/\bar{U} \qquad (21a)$$

$$n_1 = 1.408 - 0.186A/\bar{U} \qquad (21b)$$

$$\tau = 4.088\times10^{-3} - (1.193\times10^{-3})A/\bar{U}\ \text{s} \qquad (21c)$$

$$\sigma = 8.223\times10^{-4} - \left(2.905\times10^{-4}A/\bar{U}\right)\ \text{s} \qquad (21d)$$

These results have been obtained from full CFD simulations; for details, see [9]. The flame (which is modelled by a flame speed closure model) is excited numerically by a single-frequency signal, for different amplitudes and frequencies. The perturbation is applied at the inlet and the flame response is computed. Numerical derivations methods based on a multiple-frequency signals cannot be applied to such analysis since the large perturbation amplitudes induce a nonlinear flame response. These numerical FTF results were fitted using the analytical expression

$$FTF = n_1 e^{i\omega\tau_c}e^{-\sigma^2\omega^2/2} - n_0, \qquad (22)$$

which is the frequency-domain equivalent of Eq. (14). The parameters n_0, n_1, τ_c and σ were determined by a constrained least-squares method, i.e. by minimising the difference between (22) and the numerically obtained FTF.

In the following we present stability maps determined from the solution Ω_1 of (18) for a setup with the following features: $\bar{T}_1 = 300\text{K}$, $\bar{T}_2 = 2380\text{K}$, $K = 2.1\times10^6\,\text{Wkg}^{-1}\text{s}^{-1}$, S_{ratio} = 0.13 (ratio of cross-sectional areas), xj =0.16m (position of the temperature jump) and x_q = 0.21m (flame position). These parameters are kept constant, while the tube length L was treated as control parameter and varied between L=0.36 m and L=1.26 m. The velocity amplitudes A (normalized with the mean flow velocity $\bar{U}$) were in the range $0.01 < A/\bar{U} < 2$. The tube was a quarter-wave resonator with $R_0 = 1$ (rigid end at x=0) and $R_L = -1$ (open end at x=L). No losses of acoustic energy occur at these ends.

Stability maps for two different time-lag distributions are depicted in figure 2: (a) shows a Gaussian distribution with σ given by (21d), while (b) shows the case for σ=0, which represents a discrete time-lag.

(a)   (b)
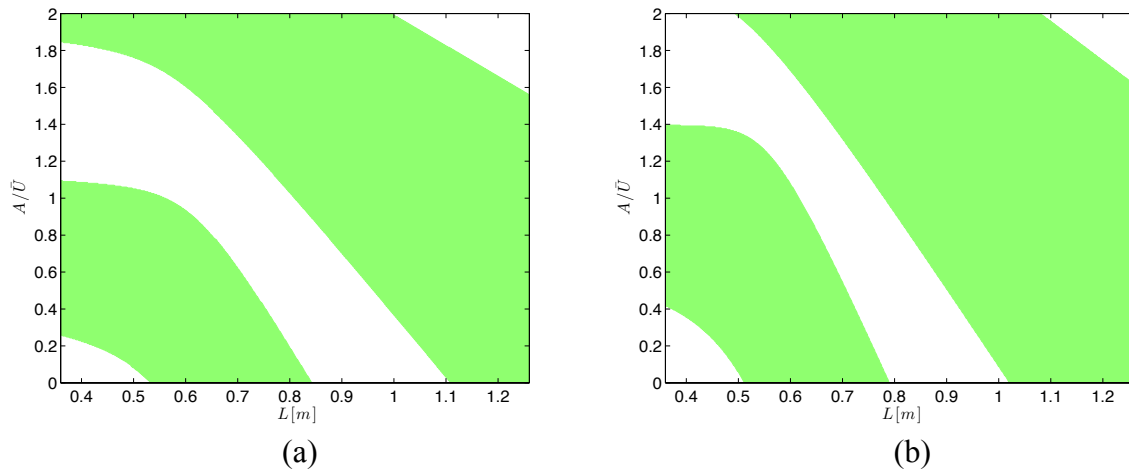
Figure 2: Stability map for the control parameter *L*. (a) Gaussian time-lag distribution. (b) discrete time-lag.

Green areas indicate regions of instability: if the combustion system is such that the pair of values $(L, A/\bar{U})$ lies in an instability region, the perturbation will *grow* until $(L, A/\bar{U})$ reaches the border with the neighbouring stable region. White areas are regions of stability: if the point $(L, A/\bar{U})$ lies in such a region, the perturbation, will *decay* in amplitude until the border with the next unstable region is reached. Interfaces between stable and unstable regions correspond to *limit cycles*: the growth rate of the perturbation is 0 for values of $(L, A/\bar{U})$ along the interfaces (see also [11]).

We observe that the presence of a time-lag distribution tends to shift the unstable regions towards lower amplitude values. There are two zones of stability for infinitesimal perturbation: 0.36 *m* <*L*<0.52*m* and 0.82 *m* <*L*<1.1*m* for the Gaussian time-lag distribution, 0.36 *m* <*L*<0.51*m* and 0.79*m* <*L*<1.02*m* for the discrete time-lag.

(a)   (b)
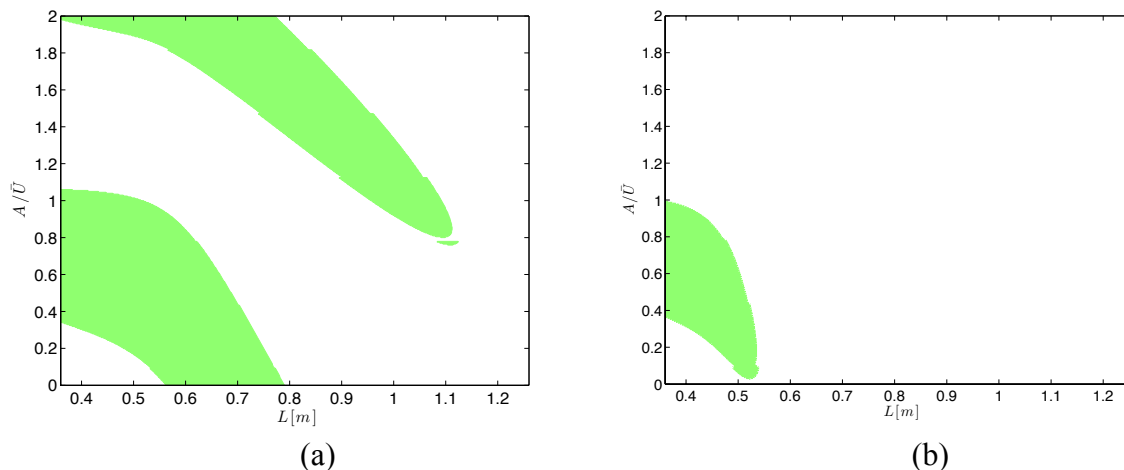
Figure 3: Stability map for the control parameter *L*. (a) open end with small losses. (b) open end with large losses.

Figure 3 shows the case where acoustic losses occur at the open end: Figure 3(a) is the stability map for small losses (R_L=-0.9), and 3(b) for larger losses (R_L=-0.576-i0.491). As expected, the size of the unstable regions decreases with losses.

Similar maps can be obtained for other control parameters, such as the heater power *K*, or the flame position x_q. However, since in the BRS burner the heater power is increased by varying the mass flow, *K* should be considered as constant.

5. Conclusion

The Green's function analysis is a mathematical tool which has a very concrete physical meaning: it is the response of the burner to an impulse excitation. This physical interpretation is very valuable. In this paper we have used a Green's function approach to describe a laboratory swirl burner in terms of actual physical modes, focussing on two effects: a time-lag distribution in the flame response, and acoustic losses at the tube ends. The physical insight gained with our approach is fundamental for the understanding and control of thermoacoustic feedback. Our approach can complement numerical methods which are computationally expensive such as Large Eddy Simulation, or Direct Numerical Simulation, providing a rapid estimation of the relevant parameter range.

REFERENCES

1 Lieuwen , T. C. *Unsteady Combustor Physics*, Cambridge University Press, Cambridge, UK ,(2012).

2 Komarek, T., and Polifke, W. Impact of Swirl Fluctuations on the Flame Response of a Perfectly Premixed Swirl Burner, *J. Eng. Gas Turbines Power*, **132**, 061503-1,7, (2010).

3 Tay-Wo-Chong, L. and Polifke, W. LES-Based Study of the Infuence of Thermal Boundary Condition and Combustor Confinement on Premix Flame Transfer Functions, ASME paper GT2012-68796, (2012).

4 Iurashev, D. Internal Report, Ansaldo Energia S.p.A., PDE/ISV/TMC/TFC, via N. Lorenzi 8, 16152 Genova, Italy, (2015).

5 Kosztin, B. *Linear and non-linear modelling of thermoacoustic instabilities in a laboratory burner*, PhD thesis, Keele University, (2013).

6 Polifke, W., Kopitz, J., and Serbanovic, A., Impact of the Fuel Time Lag Distribution in Elliptical Pre- mix Nozzles on Combustion Stability, *7th AIAA/CEAS Aeroacoustics Conference*, Maastricht, The Netherlands, 28-30 May, (2001).

7 Subramanian, P., Blumenthal, R. S., Polifke,W. and R.I. Sujith Distributed time lag response functions for the modelling of combustion dynamics, *Combustion Theory and Modelling*, **19**(2), 223-237, (2015).

8 Noiray, N., Durox, D., Schuller, T. and Candel, S. A unified framework for nonlinear combustion instability analysis based on the flame describing function, *Journal of Fluid Mechanics* **615**, 139-167, (2008).

9 Iurashev, D., Campa, G. and Anisimov, V. Response of swirl stabilized perfectly premixed flame to high-amplitude velocity excitations, *23rd International Congress on Sound and Vibration*, Athens, Greece, 10-14 July, (2016), submitted.

10 Stow, S. R and Dowling, A. P., A time-domain network model for nonlinear thermoacoustic oscillations, *Journal of Engineering for Gas Turbines and Power* - Transactions of the ASME 131, article no 03150 (2009).

11 Bigongiari, A. and Heckl, M. 2015 A Green's function approach to the study of hysteresis in a Rijke tube. *Proceedings of the 22nd International Congress on Sound and Vibration*, Florence, Italy, 12-16 July, (2015) .

12 Kornilov, V.N., Rook, R., Boonkkamp, J.H.M.t.T. and de Goey, L.P.H. Experimental and numerical investigation of the acoustic response of multi-slit Bunsen burners, *Combustion and Flame* **156**, 1957-1970, (2009).

13 Heckl, M.A. and Howe, M.S. Stability analysis of the Rijke tube with a Green's function approach, *Journal of Sound and Vibration* **305**, 672-688, (2007).

14 Heckl, M.A. A new perspective on the flame describing function of a matrix flame, *International Journal of Spray and Combustion Dynamics* **7**, 91-112, (2015).